



LEARNING FROM THE PAST TO FACE THE FUTURE: LANDSLIDES IN THE PIAVE VALLEY (EASTERN ALPS, ITALY).

**Sandro Rossato¹, Monica Ghirotti², Fabio Gabrieli³, Franz Livio⁴, Francesco Bovo³,
Lorenzo Brezzi³, Paolo Campedel⁵, Simonetta Cola³, Susan Ivy-Ochs⁷, Silvana Martin⁶,
Paolo Mozzi⁶, Alessandro Pasuto⁸, Manuel Rigo^{1,6}, Paolo Simonini³, Nicola Surian⁶,
Alfio Viganò⁵, Christof Vockenhuber⁷, Andrea Wolter⁹**

¹ Institute of Geosciences and Earth Resources, National Research Council of Italy, Padova, Italy.

² Department of Physics and Earth Science, University of Ferrara, Ferrara, Italy.

³ Department of Civil, Environmental and Architectural Engineering, University of Padova, Padova, Italy.

⁴ Dipartimento di Scienza ed Alta Tecnologia, Università degli Studi dell'Insubria, Como, Italy.

⁵ Servizio Geologico, Provincia Autonoma di Trento, Trento, Italy.

⁶ Department of Geosciences, University of Padova, Padova, Italy.

⁷ Department of Earth Sciences, ETH Zürich, and Laboratory of Ion Beam Physics, ETH, Zürich, Swiss.

⁸ Research Institute for Geo-Hydrological Protection, National Research Council of Italy, Padova, Italy.

⁹ Engineering Geology, GNS Science, Avalon, Lower Hutt, New Zealand.

Corresponding author: S. Rossato <sandro.rossato@igg.cnr.it>

ABSTRACT: Landslides are a critical process in landscape evolution and may pose a serious threat to people and infrastructure. In the last decades, a growing interest in such phenomena has developed in the Alps, where narrow valleys are increasingly inhabited, and landslides have caused several casualties. Understanding the driving factors, triggers, evolution, and impact of past and future failures is of the utmost importance when dealing with land use and risk reduction. In this paper, four distinct case studies are presented, showing how different approaches can interact and produce a comprehensive understanding of a landslide event. All examples lie in the middle sector of the Piave Valley (NE Italy) and deal with failures that occurred in the distant past (i.e., the historic Masiere di Vedana rock avalanche), in the near past (i.e., the 1963 Vajont event), in the present (i.e., the 60-years-lasting Tessina landslide) and in the future (i.e., possible Mt. Peron instabilities). The final goal of the paper is to show how the understanding of past landslides is fundamental to obtain reliable predictions on future failures, and how modelling designed to predict the evolution of potential detachments can be applied to understand the dynamics of ancient events.

Keywords: Field survey, remote sensing, modelling, land management, isotopic dating.

1. INTRODUCTION

Landslides have always been a relevant topic for both researchers and society. They are both a relevant process in landscape evolution and a severe risk to human lives and buildings. Due to the potential catastrophic consequences, landslides can be considered one of the most threatening and devastating natural hazards in densely populated mountain regions (Crosta et al., 2004; Abdulwahid & Pradhan, 2017). Dilley (2005) estimated that 66 million people live in areas classified as “high-risk”. Globally, Italy is particularly prone to landslide hazard, having vast mountainous regions and a dense network of populated areas and infrastructures, that nearly tripled in the last 70 years (ISPRA, 2018). According to the Italian landslide inventory (IFFI; Trigila et al., 2007; <http://www.progettoiffi.isprambiente.it/>),

which is designed to collect and organize all landslides in Italy, more than 600,000 landslides (i.e., about two thirds of all European events; Herrera et al., 2018) have occurred in Italy, affecting over 23,700 km², (i.e., 7.9% of the entire nation; Trigila et al., 2018). Currently, about 1,280,000 people live in areas classified as “very high” and “high” risk (Trigila et al., 2018). It is worth noting that the costliest natural disaster in Italy in the last 30 years was the 1987 Val Pola Landslide, with an estimated impact of about US\$ 400 million (Crosta et al., 2004).

When facing decision-making processes regarding the land use of their territory, administrations should take into consideration landslide hazard and vulnerability (e.g., Abdulwahid & Pradhan, 2017), and how these values may vary over time (e.g., Massey et al., 2014). Locally focused surveys and modelling, combined with

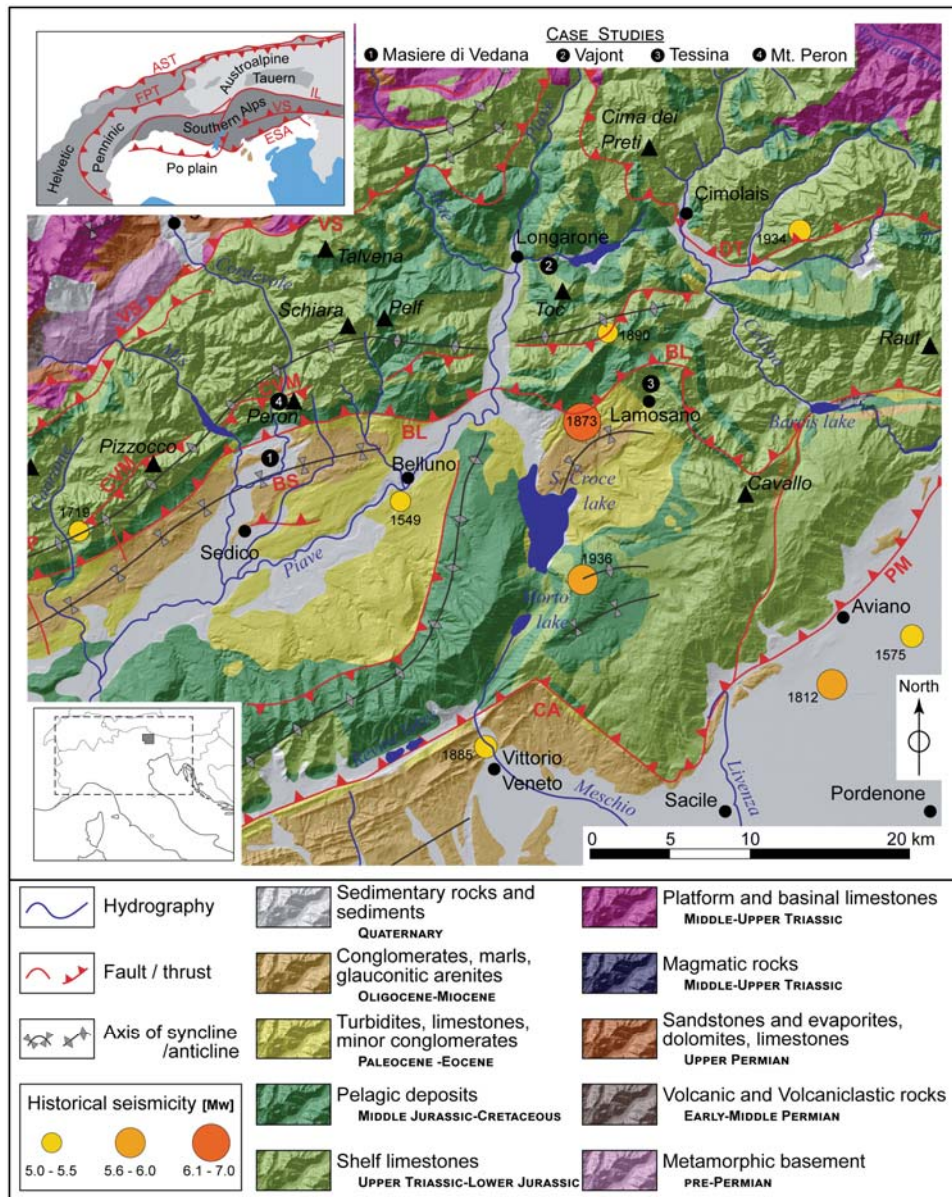


Fig. 1 - Simplified geological map of the Alpine sector with the location of the case studies (black circles). The map is based on the Structural Model of Italy (Bigi et al., 1990), the Belluno geological map (Costa et al., 1996), and the paper by Zanferrari et al. (2013) and overlies the Italian SRTM derived Digital Elevation Model (25-m cells). Small-scale structural setting (upper-left corner) is based on Doglioni (1990). AST: Alpine Sole thrust; BL: Belluno thrust; BS: Belluno syncline; CA: Cansiglio thrust; CP: Coppolo-Pelf anticline; CVM: Val Carpenada-Val di Vido-Val Madonuta thrust; DT: Monte Duranno-Tramonti thrust; ESA: eastern Southern Alps thrust system; FPT: Frontal Penninic thrust; PM: Polcenigo-Montereale thrust; IL: Insubric Line; VS: Valsugana thrust.

the investigation of past events are fundamental in the evaluation of potential failures (Samia et al., 2017). Identifying the driving factors and possible triggers is also pivotal (e.g., Eisbacher & Clague, 1984; Nicoletti & Sorriso-Valvo, 1991; Hungr, 2006; Strom, 2006; Hermanns & Longva, 2012).

Several aspects are common in large, catastrophic rockslides. First, a distinctive trigger is not always apparent or necessary. The context of the slope, such as strata folds and faults, geomorphic processes, hydrogeological conditions, and slope morphology may be suffi-

cient to damage the rock slope and bring it to failure (Donati et al., 2020). At this stage, any small change in equilibrium may cause catastrophic failure. The second aspect is the structural setting: elements such as faults, folds, and fractures play a significant role in most rock slope failures. Sliding surfaces are commonly located on planes of weakness such as bedding and foliation, where water can infiltrate, weathering can take place and failures may occur. Seismic events and hydrogeological conditions commonly act in concert with lithological and structural controls to condition slopes for failure (Stead &

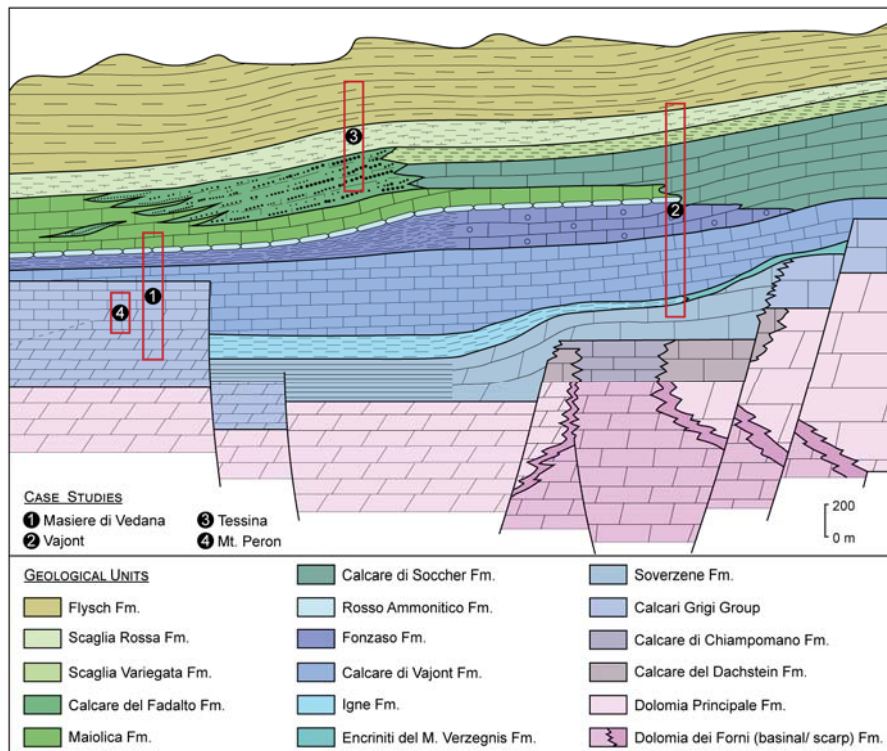


Fig. 2 - Stratigraphic sketch of the geological units cropping out in the Belluno area, based on Costa et al. (1996) and Carulli et al. (2000). The portions of the stratigraphic sequence involved in each case study is shown.

Wolter, 2015). Finally, many large rock slopes show some sign of movement prior to collapse, and some slopes continue to slowly deform after failure. This trend agrees with what Glastonbury & Fell (2010) observed when examining characteristics of large rapid rockslides. They suggested that strength loss along the rupture surface is a key element to the initiation of rapid failures. Not all slowly deforming slopes have evolved into rapid landslides, however.

In the Piave Valley, many landslides are reported, and vary remarkably in size, kinematics, and impact. Some of them are sadly known to have caused much damage and numerous casualties (Rossato et al., 2018) and the vast majority are influenced by the regional stratigraphic and tectonic setting. In the eastern Southern Alps, the indentation of the Adria plate with the Alpine orogeny deformed the entire bedrock package, folding, faulting and overthrusting the stratigraphic sequence and creating or reactivating a dense system of tectonic structures (Márton et al., 2003; D'Agostino et al., 2008).

In this paper we aim to compare approaches, data, and possible outcomes deriving from different types of landslide studies. We chose four distinct case studies, dealing with events that occurred in the distant past (i.e., the historic Masiere di Vedana rock avalanche), in the near past (i.e., the 1963 Vajont event), in the present (i.e., the 60-years-lasting Tessina landslide) and possibly in the future (i.e., Mt. Peron instabilities) (Fig. 1). Each of them will be described, highlighting the investigation methods that have been applied, the impact on

the landscape and the population, and remaining open questions. We chose these case studies to highlight how remarkably different landslides can occur in a small area. The examples have been collected in the middle sector of the Piave Valley and its surroundings, within a maximum distance of ~15 km from Belluno, the largest city of the valley. All case studies will show how an integrated approach considering multiple disciplines (e.g., structural geology, engineering geology, geomorphology) and methods (e.g., field survey, remote sensing, dating techniques, numerical modelling) is needed for effective landslide recognition and hazard assessment. The landslides discussed in this paper have been also presented in the framework of the sites visited in Trentino/South Tyrol during the Summer School on "Historic and prehistoric landslides in the NE Italian Alps - Implications for new hazard maps in mountainous areas", hosted by the University of Padua in 2019. The other sites of the Trentino region visited during the Summer School are presented in a companion paper in this volume (Martin et al., 2020).

2. SETTING

The Piave Valley is one of the largest valleys in the eastern Southern Alps. The northern sector of this valley is NNE-SSW trending and narrow (the valley bottom is ~1 km wide at Longarone), whilst near Belluno it becomes wider (~4 km) and turns towards SW (Fig. 1). The present shape of the Piave Valley is mostly due to Quaternary glacial activity. During the last glacial phase

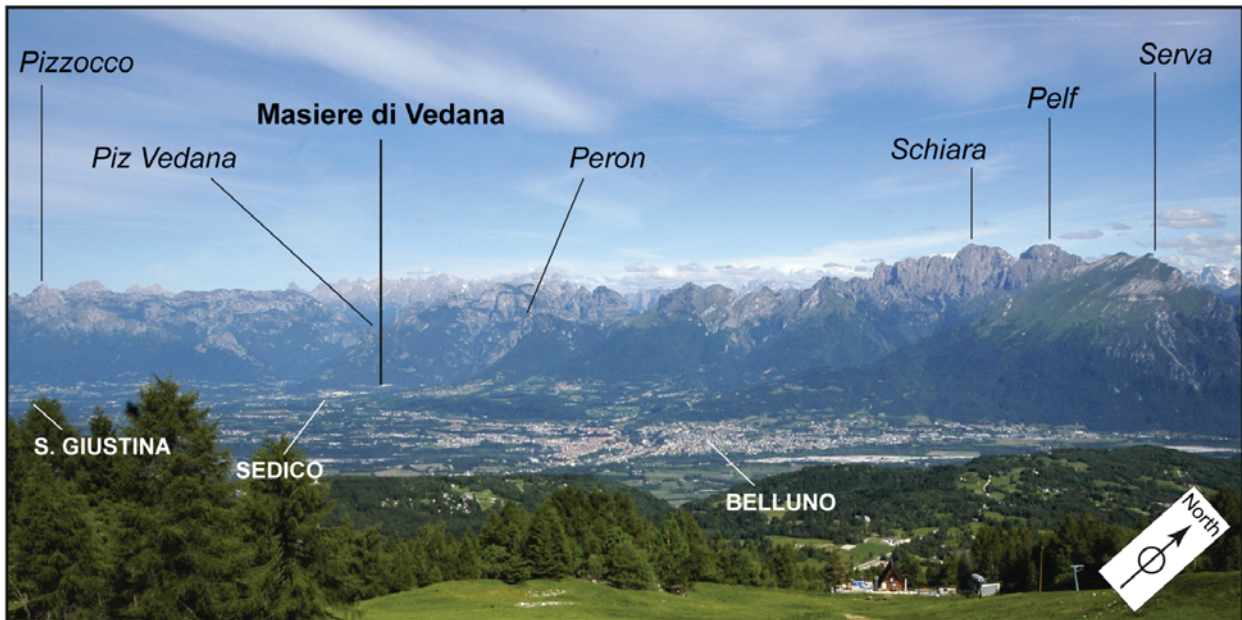


Fig. 3 - Panoramic view of the northern side of the Piave Valley, with the location of the Masiere di Vedana deposit and the major peaks and towns highlighted.

(30-17.5 ka cal BP; Monegato et al., 2017), the Piave glacier, sustained also by tributary ice-streams, was up to 1,000 m thick in the study area (Pellegrini et al., 2006; Carton et al., 2009; Pasuto, 2017). At Ponte nelle Alpi, the Piave glacier split into two tongues flowing to the SW and to the S, along the Piave Valley and the Lapisina Valley, respectively.

The study area belongs to the Neogene-Present back-thrusted (S-vergent) part of the Alpine chain. It is bounded by two of the main tectonic lineaments related to the Alpine orogeny: to the north by the Valsugana thrust fault and to the south by the S-verging and WSW-ENE oriented Belluno thrust (Doglioni, 1990; Galadini et al., 2005). All case studies belong to the hanging wall of this latter tectonic structure (Doglioni, 1990), that bounds the northern limb of the Belluno syncline. The stratigraphic sequence of the forelimb is deformed to various extents, locally even overturned (Doglioni, 1990; Costa et al., 1996).

Since the Jurassic, the study area has been characterized by the presence of a basin (Belluno Basin) bounded by two platforms, one to the east (Friulian) and one to the west (Trento). The dominant lithologies of the platforms are Triassic limestones and dolomites. In the Belluno Basin, the Jurassic and Cretaceous limestones and marls are conformably overlain by Eocene turbidites, which are in turn unconformably covered by Oligo-Miocene sandstones and clays (Venzo, 1939; Stefani et al., 2007) (Fig. 2). South of Ponte nelle Alpi, the Piave Valley separates the Alps from the Venetian Prealps, representing the forelimb of the Alpine chain, mainly made of Mesozoic and Tertiary sedimentary rocks (Costa et al., 1996).

Due to the lateral variability of the geological units, as well as the presence of minor tectonic features and peculiar deformations, each case study will include

more site-specific information.

3. THE MASIERE DI VEDANA ROCK AVALANCHE (MV)

3.1. Historical background

The Masiere di Vedana (Abele, 1974; Eisbacher & Clague, 1984; Pellegrini et al., 2006), also known as “Rovine di Vedana” (Mazzuoli, 1875; Squinabol, 1902; Montandon, 1933) or “Marocche di Vedana” (Dal Piaz, 1912; Venzo, 1939), is a blocky deposit located south of Mt. Peron (1486 m a.s.l.), 8 km west of Belluno (Figs. 1, 3).

This deposit is one of the biggest landslide deposits in the Alps (Heim, 1932; Abele, 1974; Eisbacher & Clague, 1984), covering an area of about 9 km², having a maximum thickness of 40 m and an estimated volume of more than 100 Mm³ (Abele, 1974; Genevois et al., 2006; Pellegrini et al., 2006). Many researchers dealt with this deposit in the past. The Masiere di Vedana was interpreted to be Lateglacial (Pellegrini et al., 2006) to historic in age (Piloni, 1607; Miari, 1830; Rossato et al., 2020). Even its origin was debated; it has been suggested to be: i) a glacial deposit (Hoernes, 1892), ii) landslide debris transported by a glacier during the Lateglacial (Mazzuoli, 1875; Squinabol, 1902; Dal Piaz, 1912; Venzo, 1939; Pellegrini, 2000; Pellegrini et al., 2006), iii) a catastrophic flood deposit (Taramelli, 1883) and iv) a complex rock avalanche (Genevois et al., 2006; Rossato et al., 2020).

A recent study combining geomorphological and stratigraphic evidence, cosmogenic dating and literature review finally defined the Masiere di Vedana as a rock avalanche that occurred between late Roman times and the early Middle Ages (Rossato et al., 2020).

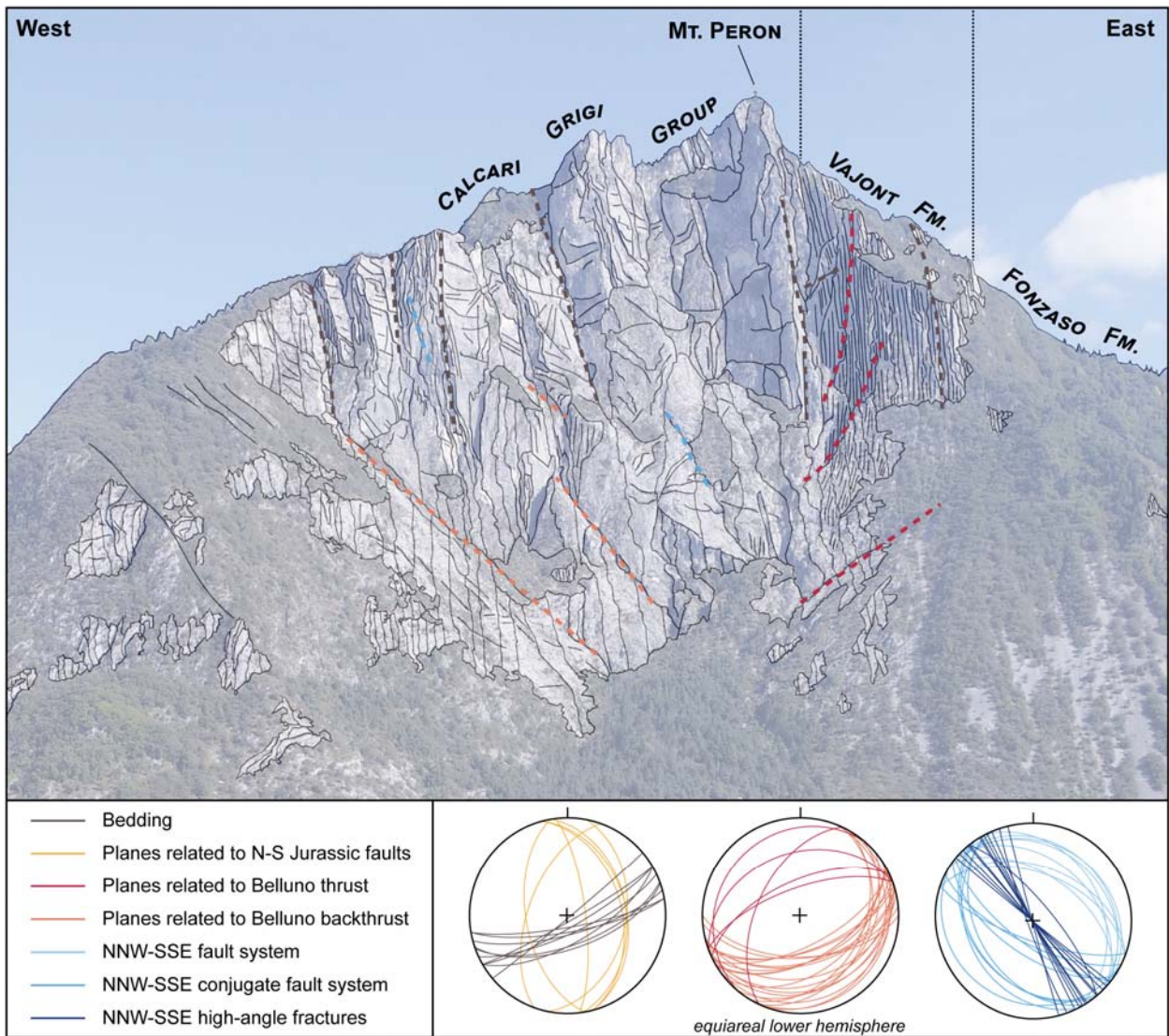


Fig. 4 - Structural scheme of the Mt. Peron main scarp, on its southern side. The main frame is a photograph (shot from Vedana sector towards the north-east, see Fig. 5 for location) with major structural elements and morphologic features highlighted. The frame below hosts the lower hemisphere stereographic projection of principal structural elements. Colours in the frames correspond to the same systems.

3.2. Setting

The rock mass detached from the southern side of the Mt. Peron (1486 m a.s.l.). This peak is part of the ENE-WSW oriented Coppolo-Pelf anticline and belongs to the hanging wall of the Belluno thrust, which crops out at the base of its southern rocky wall. The landslide crown area comprises, from west to east, Calcari Grigi Group (Lower-Middle Jurassic), Calcare di Vajont (Middle Jurassic), Fonzaso Formation, Rosso Ammonitico (Upper Jurassic) and Maiolica (Cretaceous) limestones. The strata are sub-vertical to slightly overturned (Doglioni, 1990; Costa et al., 1996). The main scarp is partially circular, 800 m wide and 700 m high, S-to-SW facing.

Mt. Peron is dissected by a wealth of fractures and faults, that can be grouped into five main discontinuity sets. These comprise: (1) bedding, (2) WSW-ENE di-

rected frontal thrust planes, (3) SE dipping backthrust-related planes, (4) NW-SE aligned local conjugate fracture planes sets, and (5) persistent N-S oriented planes (Fig. 4; Rossato et al., 2020). Presently, myriad large and small individual rock prisms bounded by these discontinuities are present at high elevation in the crown area (Di Giusto, 2012).

3.3. Landslide kinematics and characteristics

The plain south of Mt. Peron is covered for ~9 km² by rock avalanche deposits, corresponding to an estimated total debris volume of ~170 Mm³ (detached rock mass: ~130 Mm³) (Rossato et al., 2020). The deposit is lithologically zoned, the rocks found in the proximal sectors corresponding to geological units outcropping in the western part of the detachment area (i.e., Calcari Grigi Group), while the more distal ones mimic the strati-

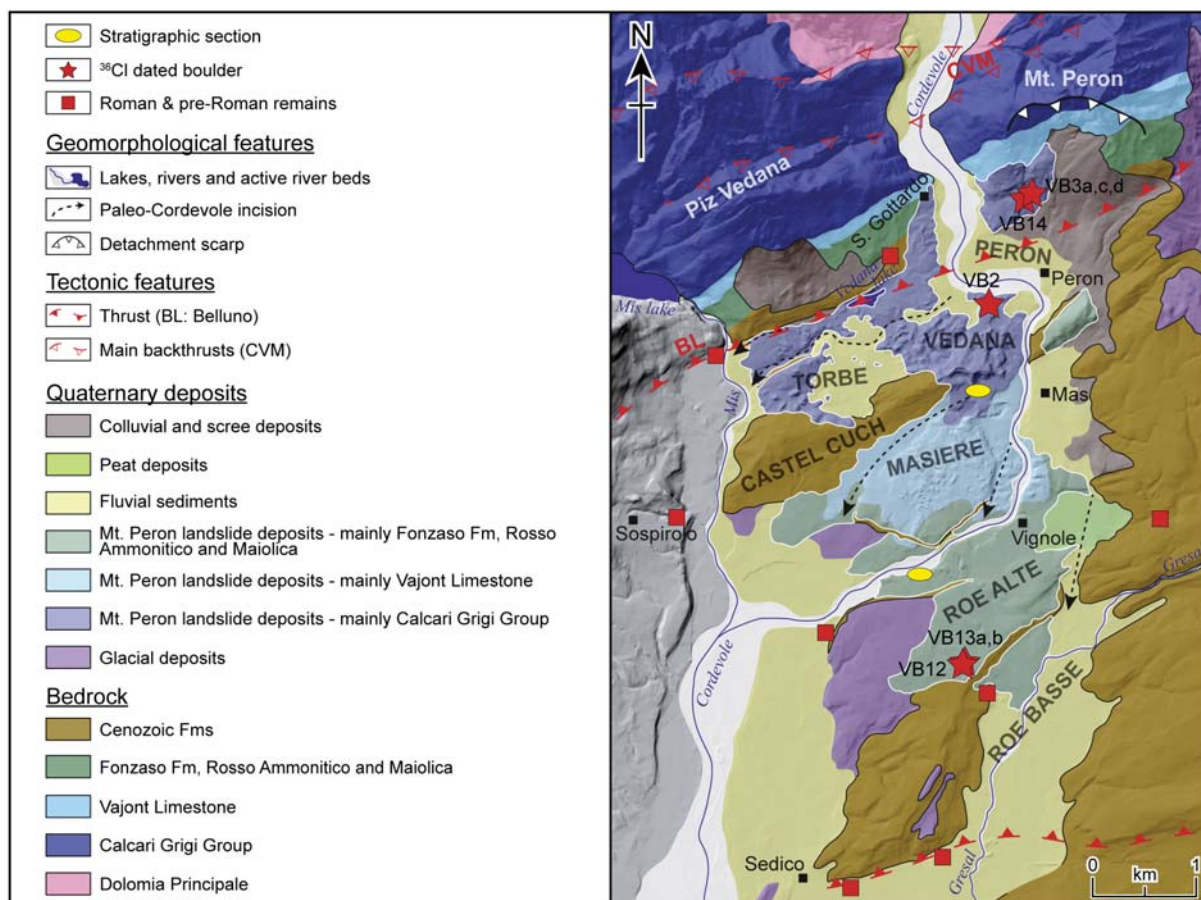


Fig. 5 - Geological map of the Masiere di Vedana, see location in Fig. 1. The boundary of Mt. Peron rock avalanche deposits is marked with solid white line, whilst the contact between Quaternary sediments and bedrock is shown with solid black line. The location of boulders sampled for dating (red stars) are shown. Archaeological findings are indicated by red squares. Location of stratigraphic sections (yellow ellipses) and paleo-Cordevole paths (black dashed arrows) are shown. (Modified from: Rossato et al., 2020)

graphic sequence of the eastern side (i.e., Calcare del Vajont, Fonzaso, Rosso Ammonitico and Maiolica Formations). The mobility of rock avalanches depends strongly on the involved volume, especially in non-confined setting (Strom, 2006). The Masiere di Vedana rock avalanche travelled about 5,900 m, a distance that can be achieved only hypothesizing a single massive failure. The calculated H/L ratio of ~ 0.2 (Fahrböschung angle of 11°) (Rossato et al., 2020) marks this event as extremely mobile, compared to other rock avalanches (Aaron & McDougall, 2019). The Masiere di Vedana rock avalanche ran only partially over Cenozoic rocks and Pleistocene conglomerates, the vast majority of the path material being constituted by alluvial and glacial deposits, with scattered humid sectors (Fig. 5; Rossato et al., 2020). The presence of loose, saturated substrate like that described for the Masiere di Vedana event is proved to favor longer travel distances, thinner debris tongues, and wider debris distribution (Aaron & McDougall, 2019).

Based on spatial pattern, boulder lithology and morphological character, we distinguish five sectors of the deposits: Peron, Vedana, Torbe, Masiere, and Roe (Roe Alte and Roe Basse) (Fig. 5).

- The **Peron** sector includes the talus apron deposits at the foot of Mt. Peron, the rock avalanche deposits on the east side of the river and the terrace of Peron town (at about 380 m a.s.l.).
- In the **Vedana** sector, the rock avalanche deposit displays a highly irregular, thinly forested topography with huge blocks hundreds of cubic meters in size. Locally, glacial sediment is incorporated into the base of rock avalanche.
- The **Torbe** sector encompasses the distal rock avalanche deposits of the lobe north of Castel Cuch where isolated conical hills and hummocks ("toma"; More & Wolkersdorfer, 2019) emerge from a flat topography. In the flat area a few meters of silty sands cover the rock avalanche deposits, likely due to fluvial deposition by the Cordevole River.
- The **Masiere** part is a vegetation-free, desert-like expanse of limestone blocks. Boulders are meter-size and abundant angular and sub-angular clasts, lacking fine matrix in the surficial deposits.
- The areas of **Roe Alte** and **Roe Basse** comprise the distal sector; very few boulders immersed in a sandy matrix are scattered in the meadows. The Roe Basse sector is made of alluvial sediments which

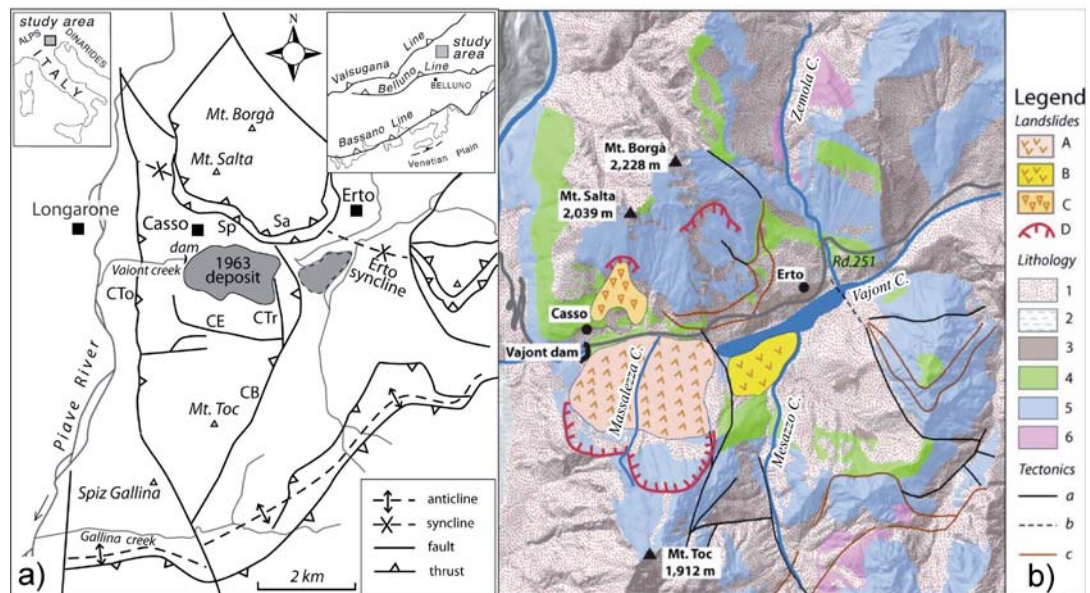


Fig. 6 - a (left): Structural sketch of the Vajont area (modified after Riva et alii, 1990). b (right): Geomorphological sketch map of the Vajont Valley. Legend: A Vajont Landslide; B La Pineda Landslide; C Salta rock fall; D landslide scarp; 1 slope deposits; 2 fluvial deposits; 3 marls, marly limestones and flysch (Marne di Erto and Flysch Formation, Palaeocene p.p.-Eocene); 4 reddish and nodular limestones, white micritic limestones (Rosso Ammonitico, Maiolica, Scaglia Rossa, Lower Cretaceous-Lower Palaeocene p.p.); 5 white oolitic and bioclastic calcarenites, grey dolomitized micrites and limestones with interlayers of thin clays (Soverzene Formation, Igne Formation, Calcarea di Vajont Formation and Fonzaso Formation, Jurassic); 6 white or grey massive dolomite (Dolomia Principale, Upper Triassic); a fault; b uncertain fault; c overthrust (from Pasuto A., 2017).

mantle the rock avalanche deposit on the northwestern side. Locally, the rock avalanche shows direct and sharp basal contact with glacial sediment.

Pore pressure increase and seismic shaking are the principal contenders when trying to identify the actual trigger of failure in rock avalanches, that may even start without a definite external event (Wieczorek, 1996; Schuster & Wieczorek, 2002; Takahashi, 2001).

The area near Belluno has a high mean annual rainfall (1643 mm in the time interval 1994-2018; <https://www.arpa.veneto.it/dati-ambientali/open-data>) and extreme rainfall events are recorded, even in recent times (e.g., >300 mm of rain at Sospirolo during a single event: 27th October - 1st November 2018; ARPAV, 2018). Severe rainfall periods occurred also at the time of the event (Wirth et al., 2013; Rossato et al., 2015) and may have triggered, or have contributed to, the Masiere di Vedana rock avalanche.

The Veneto region is susceptible to seismic activity and has experienced several major earthquakes in the last few hundred years, some up to Mw 6. A couple of historic earthquakes occurred in the time frame of the Masiere di Vedana, but no direct relationship is proved. However, an important consequence of frequent seismic activity is the decrease of mechanical properties of the rock mass, with the propagation of failure planes and the reduction of roughness on discontinuities (Friedmann et al., 2003; Brideau et al., 2009; Parker et al., 2013; Stead & Eberhardt, 2013; Preisig et al., 2015; Gischig et al., 2016).

The Masiere di Vedana rock avalanche may have been triggered by an exceptional meteorological event, an earthquake, or a combination of them. Nevertheless,

no exceptional event may be required for such rock avalanches to occur, as the accumulation of damage markedly lowers the energy needed to trigger a failure (Rossato et al., 2020). The rock mass likely moved at the beginning as toppling and/or sliding, evolving into a flow-like movement of crumbling rock debris, extremely variable in size (from clay/silt up to plurimetric boulders) and remarkably mobile (Rossato et al., 2020). Numerical modelling suggests the presence of high pore water pressures (Genevois et al., 2006), further enhancing the mobility of the moving mass, that traveled for some kilometers and overcame obstacles such as the Castel Cuch ridge (Fig. 5), as rock avalanches typically do (e.g., Hungr et al., 2001; Mangeney et al., 2010; Bowman et al., 2012).

Today, numerous partially detached rock prisms are evident along the upper part of the Mt. Peron rock wall. As the same predisposing factors that likely led to the rock avalanche (pervasively fractured rock, vertical strata, fracture planes cutting the stratigraphic sequence) and triggers (seismicity and/or extreme rainfall events) are still present, a re-evaluation of the landslide hazard may be necessary.

4. THE 1963 VAJONT LANDSLIDE (VJ)

4.1. Historical background

The 1963 Vajont landslide, located in the Vajont Valley (Fig. 1) is one of the best-known examples of disasters caused by human activity. The Vajont double arch dam stands 261.6 metres above the valley floor and was the world's highest thin arch dam when it was built. The planned full reservoir capacity was 169 million

m³. On October 9th, 1963, during the third filling of the reservoir, a mass of approximately 270 million m³ detached from the northern side of Mt. Toc and slid into the water at velocities up to 30 m/s. A wave subsequently overtopped the dam by 250 m and swept into the Piave Valley below, resulting in approximately 2,000 deaths. The sliding lasted less than one minute and produced seismic shocks, which were recorded throughout Europe. Remarkably, the dam remained intact: it withstood a load eight times greater than that it was designed to withstand.

4.2. Setting

The Vajont Valley coincides with the core of an Alpine syncline (Erto syncline) with an E-W to WNW-ESE trending axis gently plunging towards the E. The Erto syncline lies on the hanging wall of the Belluno thrust and is paired with the trailing limb of a main frontal asymmetric anticline located to the south.

The sliding layered sequence was laterally constrained by a system of subvertical faults (Croda Bianca and Col Tramontin Lines to the east and west branch of the Col delle Erghene Line to the west), while the crown was constrained by E-W striking structures (Col delle Erghene Line) (Fig. 6a). The landslide involved Jurassic and Cretaceous rocks (limestones and marls belonging mainly to the Calcare di Soccher, Rosso Ammonitico, and Fonzaso formations) showing varying degrees of fracturing.

In the Vajont Valley and adjacent mountain groups, geological formations range in age from the Upper Triassic (Dolomia Principale) to the Middle Eocene (Flysch) (Figs. 2, 6b). They are mainly represented by limestones and dolostones. Here, several huge landslide accumulations of different age and size are present (Fig. 7) (Ghirotti et al., 2020). The most impressive one is certainly that related to the October 1963 catastrophic landslide.

4.3. Landslide kinematics and characteristics

During the third reservoir filling operation, the northern slope of Mt. Toc failed suddenly over a length of 2 km and a surface area of 2 km². The slide displaced a 250 m thick mass of rock some 300 to 400 m horizontally with an estimated velocity of 20 to 30 m/s, before running up and stopping against the opposite side of the Vajont Valley. The majority of the slide moved as a whole and reached the opposite side of the valley without any change in shape apart from a general rotation evident from both the surface morphology and the stratigraphic sequence that remained essentially unchanged after the movement (Fig. 8). It is remarkable that the Massalezza Creek, that was flowing from Mt. Toc before the event, did not change much its path and is still flowing longitudinally across the fallen mass (Fig. 6b). In 1960, F. Giudici and E. Semenza discussed the geology in detail and put forward the hypothesis of the existence of a very old landslide on the left bank of the



Fig. 7 - Drone photo of the main landslide body.

Vajont reservoir area. During their surveys they discovered a highly fractured zone ("mylonite") extending about 1.5 km along the left side of the valley corresponding to the terminal sliding plane of a prehistoric landslide (Semenza & Ghirotti, 2000). Nevertheless, the dam owners concluded that a deep-seated landslide was very unlikely to occur, mainly because of the good quality of in situ rock masses, as derived from seismic surveys and drillings.



Fig. 8 - Aerial photograph taken a few days after the landslide (photo: Selli et al., 1964). This picture clearly shows the vegetated tails of the two main lobes. The surviving vegetation highlights that these areas were not affected by the returned wave displaced by the landslide. The trees moved downslope approximately 600 m and were rotated uphill. The red circle indicates the "Bosco Vecchio".

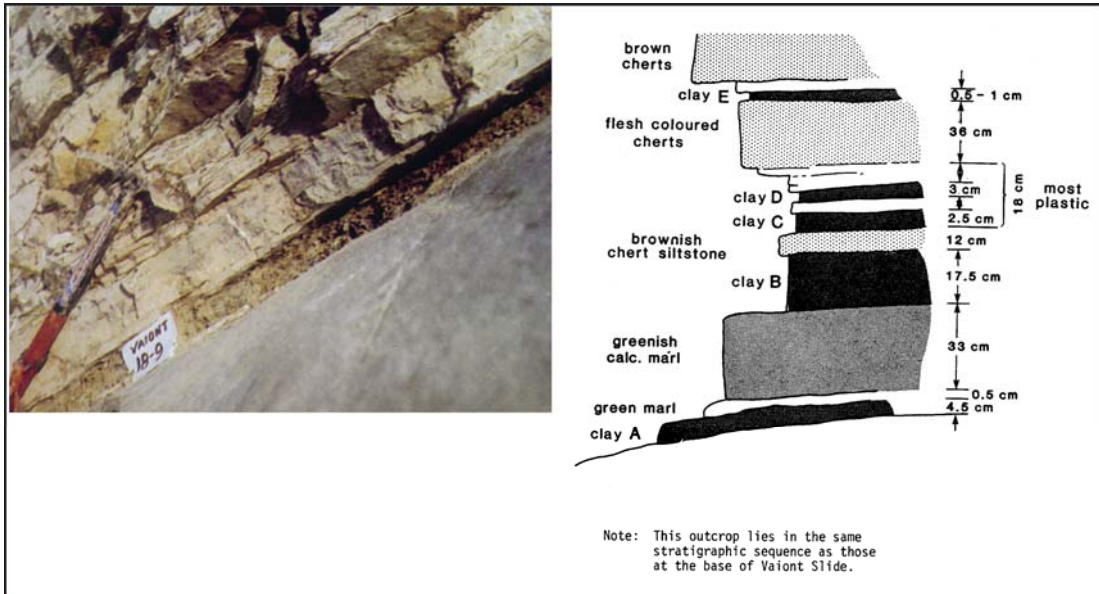


Fig. 9 - Clay interbeds outcropping on the sliding surface (at left) and a sketch of the Fonzaso Fm. outcrop southwest of Casso (adapted from Hendron & Patton, 1985).

Today, it is almost unequivocally accepted that the 1963 failure occurred mostly along planes of weakness represented by 0.5-18 cm thick clay-rich layers (Fig. 9) within the Fonzaso Formation (Hendron & Patton, 1985). However, the continuity and the existence itself of clay interbeds in the calcareous sequence and the hypothesis of a paleolandslide represented a controversial aspect for many decades. Hendron & Patton (1985)

stated that the increase in pore water pressure due to the raising of the water level in the reservoir caused a decrease in effective normal stress, favouring the sliding on these clay layers characterised by a residual friction angle ϕ_r , between 8° and 10° .

Movement occurred along a circular to chair-shaped failure surface at or close to residual strength (Fig. 10), which is hypothesized to be either a reactiva-

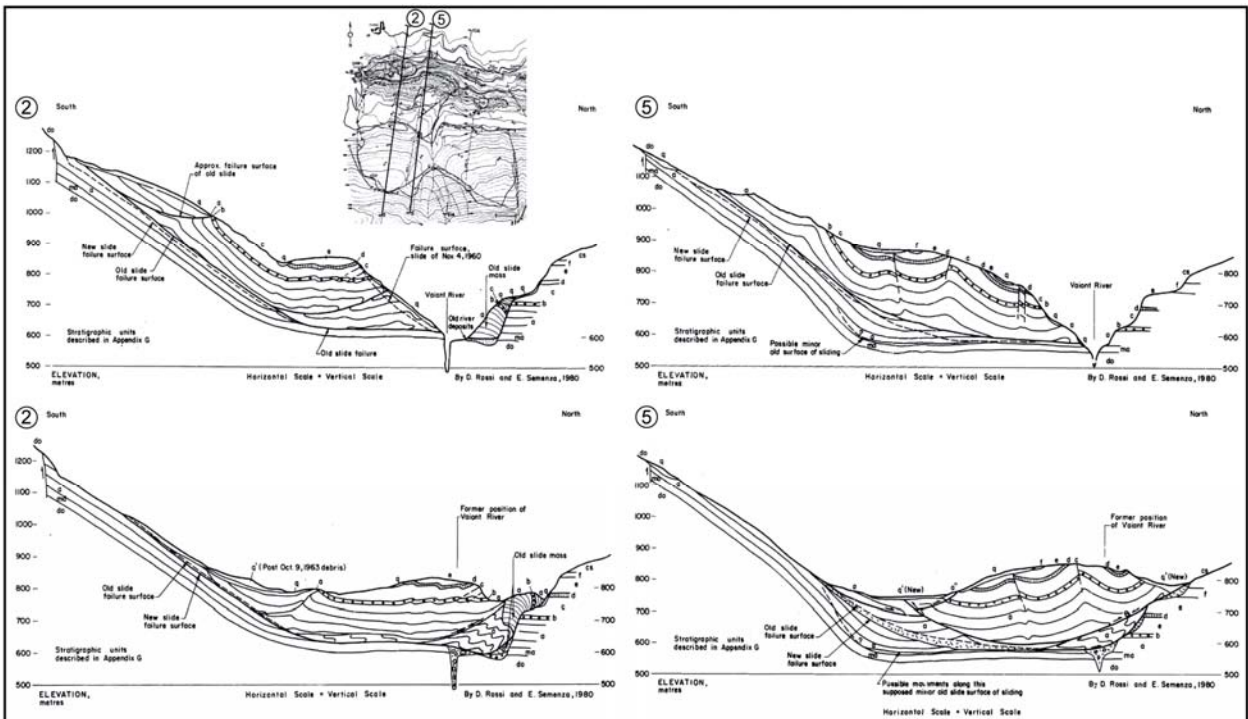


Fig. 10 - Geological sections before and after October 9, 1963 (Hendron & Patton, 1985, section 2 and 5).



Fig. 11 - Morphologies of the sliding surface (eastern lobe at left and western lobe at right).

tion of a paleo sliding surface (Semenza & Ghirotti, 2000; Semenza, 2010) or have evolved from deep-seated gravitational movement over millennia (e.g., Wolter et al., 2016). According to some authors (Dykes & Bromhead, 2018a; 2018b), there is no paleo landslide at all. The stratigraphic sequence remained essentially unchanged after the movement and the deposit has preserved, after the slide, the main systems of discontinuities and folds present before 1963. Some major vertical fractures were formed during failure, and the pre-existing sets were rotated according to the direction of the movement. Geological and tectonic evidence suggests that the landslide was limited by one or more faults (Massironi et al., 2013).

The sliding plane has an overall concave shape with the eastern and western (i.e., the lateral) lobes converging toward Massalezza Creek (Fig. 6b), which coincides with the hinge of the Massalezza Syncline. The result is that the Vajont failure surface is neither sharp nor smooth. The most tectonized sector of the sliding plane is downstream of Massalezza Creek where the hinges of the Erto and Massalezza synclines interfere with each other. The orientation of the failure surface is the product of at least two episodes of folding, which formed the multiple steps that are observed on the failure surface. All of these elements, mainly predating any gravitational event on the Mt. Toc northern slope, may have played a significant role in failure behaviour. The Massalezza Syncline and related concave shape of the sliding surface played a major role in the evolution of the 1963 Vajont landslide, favouring the collapse of the two main lobes (eastern and western) that followed two slightly different and northward converging sliding paths. As regards the failure surface morphology, important differences, moving from west to east along it are present (Fig. 11; more details can be found in Wolter et al., 2014; 2016): the western area has a “chair-like” shape and is much smoother than the central folded area. It is marked by one large and several smaller steps, as well as conjugate discontinuities; but the failure surface remains, more or less, in the same stratigraphic interval that contains the clay-rich levels (Fonzaso Fm.). The central part of the sliding

surface, incised by the Massalezza Creek, is highly tectonized and characterized by the presence of a large fold with smaller parasitic folds along its limbs. The eastern sector, limited by the Col Tramontin (CTr) fault (Figs. 6, 10), has a pronounced convexity and an irregular shape: moving from Massalezza Stream towards east, multiple steps with different strikes allowed the failure surface to rise in the stratigraphic sequence. The CTr Fault represents the eastern boundary of the 1963 slide to which Hendron & Patton (1985) attributed about 40% of the total resistance of the landslide mass. The CTr Fault also prevented the propagation of the landslide eastward because, east of it, the Fonzaso Fm., in which most of the failure surface developed, and the overlying Calcare di Soccher Fm. that forms the 1963 accumulation body, actually dip sharply northward and therefore do not outcrop in the Vajont gorge. The CTr Fault also represented a permeability boundary that could affect the groundwater flow system of the landslide mass. Hydrogeological investigation, yet to be completed, might clarify the question and lead to a reliable hydrogeological scheme of the area.

The Vajont landslide has a very rich scientific literature (Superchi et al., 2010). Still today some authors deny the existence of the paleo landslide (Dykes & Bromhead, 2018a; 2018b) while others try, through the use of numerical models and new techniques, to construct an evolutionary geological model of one of the most complex and destructive landslides that have ever occurred (Paronuzzi & Bolla, 2012; Wolter et al., 2013, 2016; Franci et al., 2020a, 2020b).

5. THE TESSINA LANDSLIDE (TS)

5.1. Historical background

The Tessina landslide has been evolving continuously since 30 October 1960, when, following intense and continuous rainfall (398.7 mm up to that day), a 300 m long, 100 m wide, and 20 m thick front detached from the slopes of Mt. Teverone (Fig. 1). Further activations were documented up to the present day and now the landslide has enlarged to an area of more than 550,000 m², becoming one of the most active landslides in the

Eastern Italian Alps. The landslide can be divided into three different geomorphological zones (Fig. 12): an upper source area that is characterized by rotational slides and intense disruption, a collector channel where the fractured material is progressively remoulded and infiltrated by water turning into a mudflow, and a lower accumulation channel where the mud flows reach down to the villages of Funes and Lamosano. The landslide extends between the elevations of 1220 and 625 m a.s.l. and has a total length of almost 3 km and a maximum width of about 500 m. It has been used as a “natural laboratory” to test innovative monitoring systems, given its extent, several optimal monitoring points, and continuous reactivations (Avolio et al., 2000; Mantovani et al., 2000; Hervas et al., 2003; Tarchi et al., 2002; Cola et al., 2016; Gabrieli et al., 2016).

5.2. Setting

In the Tessina basin, the Flysch Formation is faulted and folded, partially eroded, and bounded to the north by the highly fragmented limestone mass (Calcarea del Fadalto; Jurassic-Cretaceous) of Mt. Teverone (Figs. 2, 13). Thin (1-2 m) outcrops of marl and marly limestone Scaglia Rossa (Cretaceous-Palaeocene) are visible at the base of the mountain, where they are irregularly interposed between the steep cliffs of Mt. Teverone and the highest scarps of the landslide. The Scaglia Rossa is distinguishable along the upper border of several scarps due to its rose colour and marks the beginning of the unweathered flysch in the upper part of the source area. Moraine deposits cover the Flysch to the NW (Moda) and NE (Roncadin and Pian de Cice) of the landslide, while other surficial Quaternary deposits were mobilized by the landslide in the past and mixed with the shallow, loosened flysch.

5.3. Landslide kinematics and characteristics

The main predisposing factor of Tessina landslide is the presence of the Flysch Formation, a stratified sedimentary unit (middle Eocene) that is 1000-1200 m thick and mainly composed of sandstone, low-permeability marl, and clays.

A secondary predisposing factor is the tectonic setting: the rainfall and snowfall infiltrating into the carbonate massif of Mt. Teverone are then conveyed



Fig. 12 - Aerial view of the landslide in 1995 (source: IRPI archive): the crown area, object of photographic monitoring, to the main collector channel and the lower deposit.

through sub-vertical fractures in the Flysch (less permeable) towards the landslide body (Fig. 13). Evidence of this behaviour is the numerous springs, sometimes under a perennial regime. A drainage tunnel built in the 1990s in the carbonate massif of Mt. Teverone had the effect of smoothing out the flow peaks but did not eliminate these springs, nor significantly reduce the activity of the landslide.

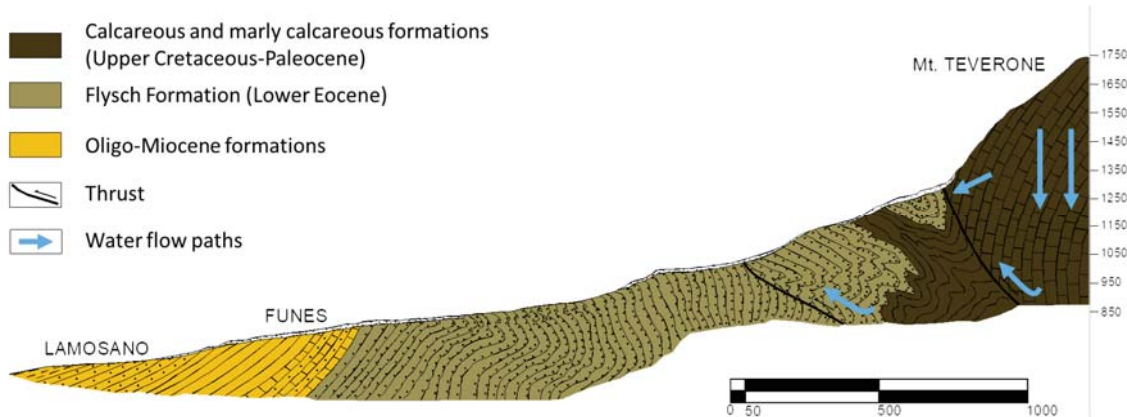


Fig. 13 - Schematic geological profile along the thalweg of the Tessina valley (adapted from Cola et al. 2016).

The third driving and triggering factor is related to the pluviometric regime of the area: according to 20 years of hourly rainfall data (1994-2014; San Martino weather station, located about 40 km to the west) the mean annual precipitation is 1683.3 mm, with an average of 121 rainy days a year and a slight bimodal seasonality with peaks in November (203.1 mm) and spring. This is one of the rainiest areas of the Veneto Region. Moreover, through photogrammetric observations (Gabrieli et al., 2016) the close link between seasonal monthly movements and cumulative precipitation has been demonstrated (Fig. 14). Such a connection has been observed and described with a similar approach also in other cases involving large debris volumes (e.g., the Super-Sauze landslide in the South French Alps; Travelletti et al., 2012), or smaller, but very active, erosion forms such as gullies (e.g., the gullies in the Guadalentín Basin in the Province of Murcia, Southeast Spain; Marzloff & Poesen, 2009).

A landslide dating back to before the triggering of the current slide in 1960 was identified by analysing multitemporal aerial photographs and digital elevation models (Van Westen & Lulie Getahun, 2003). After the first large rotational slide occurred in October 1960, ~1 million m³ of weathered flysch and Quaternary deposits were mobilised and reached the villages of Funes and Lamosano downstream. In the following years, other reactivations caused the Tessina Valley to be filled with a 30-to-50 m thick deposit (Pasuto & Silvano, 1995). The landslide deposit reached the same elevation of the village of Funes, once located on a promontory. Landslide activity seemed to decline until 1987 when several movements in the mudflow channel were documented. A further 2.5 million m³ of material mainly composed of Flysch, glacial sediments and scree deposits located in the northeast sector of the source area were reactivated in 1992 and 1995 after a rainy period, causing the damage of some infrastructures and increasing the level of risk for the villages below (Pasuto & Silvano, 1995).

While the activity of the oldest source section in the north-west seemed to decrease from 1969 to 1980, the central and eastern part discharged material with increasing frequency. The landslide is still active both in the crown area and in the side scarps with movements related to rainfall and underground water flows (Mantovani et al., 2000; Cola et al., 2016). The presence of a low-permeability retaining structure in the Flysch Formation below the depletion basin, which periodically fills with water-saturated material, seems to play a role in the intermittent dynamics of the landslide movements (Dall'Olio et al., 1987).

Different numerical modelling techniques like cellular automata (Avolio et al., 2000) and smooth particle hydrodynamic integration method (Cola et al., 2008) have been used to simulate the runout phase from the upper basin. Moreover, thanks to recent photogrammetric monitoring activity it was possible to study the worm-like movement of the mudflow from a probabilistic point of view and to examine in depth the mechanism of the movement (Gabrieli et al., 2016; Cola et al., 2019).

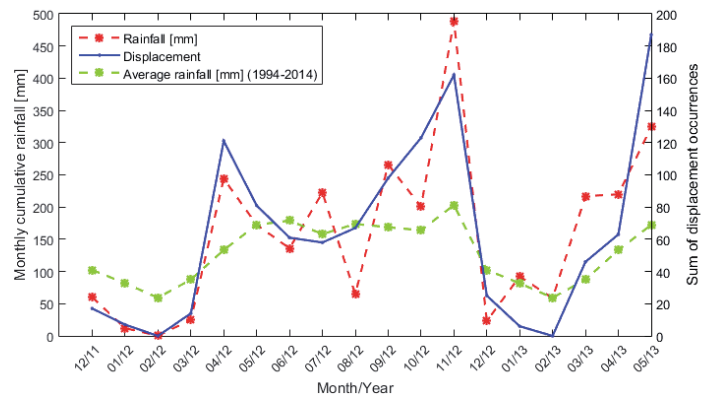


Fig. 14 - Monthly cumulative rainfalls and displacement occurrences captured from automatic photogrammetric monitoring from December 2011 to May 2013 (adapted from Gabrieli et al. 2016).

6. THE MT. PERON POSSIBLE INSTABILITIES (MP)

6.1. Setting

The Mt. Peron (Figs. 1, 15) presents as a very well exposed scar, about 800 m wide and 800 m high, sub-vertical and represented by a rocky cliff almost inaccessible to field-based measurements due to the absence of trails on the mountainside. In the scar area, many potentially unstable blocks are present, threatening the Peron village, at the base of the cliff. Some structural data have been collected in the adjoining sectors, thanks to traditional field survey and observations, and to a structural transect surveyed along a vertical rappelling descent route. With the aim of increasing the number of measurements, we tested the possibility to integrate field data with structural measurements taken on a virtual 3D model, reconstructed through photogrammetric techniques applied to a photographic survey acquired by an unmanned aerial vehicle (UAV). This work focused on an area located at the top of the landslide scar, in the western side (Fig. 15). Here, the rock mass is made of Lower Jurassic limestones belonging to the Calcarei Grigi Group (Fig. 2). The 3D model was built with 145 photos taken using a commercial UAV (Phantom 4 by DJI). From those images a point cloud of more than 6 million points, with an average spacing of 10 cm (Fig. 16a) has been built by means of the Structure from Motion and Multi-View Stereo technique (SfM-MvS; e.g., Westoby et al., 2012), through the software Agisoft Metashape[®]. Orientations of 159 planes (bedding and fractures) were measured and analysed in order to recognize clusters of fractures (i.e., fracture sets).

Figure 16b shows the 4 sets of discontinuities observed over the mountain side and the stereographic plot of the poles of those planes.

6.2. Fracture measurements in the 3D model

Fracture orientations were statistically analyzed and clustered in sets by means of the software Wintensor v.5.8.8 (Delvaux & Sperner, 2003; http://damiendelvaux.be/Tensor/WinTensor/win-tensor_download.html). First, we clustered the poles to the fracture planes through a K-means algorithm (MacQueen, 1967): the number of clusters is fixed a

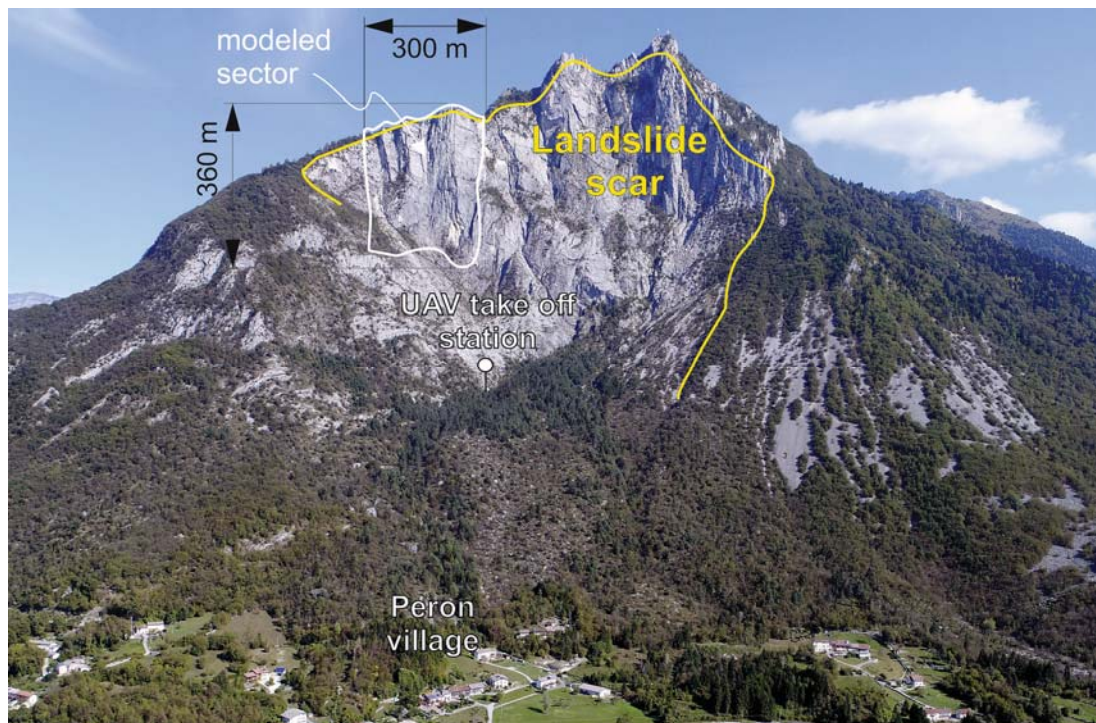


Fig. 15 - Aerial view of the Mt. Peron crown (view from the south); the area included in the virtual outcrop, south facing and near vertical, with its dimensions, the take-off location of the UAV and the area reconstructed in 3D by means of a photogrammetric approach.

priori by the operator and the calculator finds the centroids of the clusters that minimize the total intra-cluster variance and maximize the inter-cluster distance. Number of clusters were fixed with a visual inspection of the data, aided by density contouring of fracture poles. The output includes the orientation of the fracture sets, the Fisher's dispersion factor (i.e., K value) and the mean cone angle (MCA) enclosing the data distribution.

We have recognized four sets of fractures (i.e., S0, K1, K2 and K3; Fig. 16b) with 18 random discontinuities, not belonging to any set. The first cluster, S0, represents the bedding, corresponding to sub-vertical planes striking ca. WSW-ENE. The cluster K1 represents a principal sub-vertical fracture system, NW-SE-striking, that cuts through the bedding. Clusters K2 and K3 represent two secondary and less pervasive discontinuity systems. The four detected fracture sets have been compared with field-based measurements, taken at the base of the rock cliff and along a rappel descent on the same sector of the three pillars and during a field survey in close sectors of the Mt. Peron sides. Both the datasets are well matching and provide a common interpretative model.

The bedding, together with the other high-angle discontinuity (i.e., K1), provide the more pervasive fractures leading to the fragmentation of the rock mass into potentially unstable pillar-like blocks bounded at the base mainly by the K2 and K3 sets. The analyzed area is lacking significant south-dipping discontinuities, potentially favorable to the cliff instability. Nonetheless, a field survey at the base of the rock cliff highlighted the presence of a moderately dipping fault zone (i.e., the Mt. Peron backthrust; Fig. 16d) that could be a slipping sur-

face for the rock cliff described above. The presented data are essential for modeling possible failures and for a conscious and prudent management of the area by the stakeholders (e.g., the municipality of Sedico, to which the village of Peron belongs; Figs. 5, 15). The volume of the detaching rock masses, the travel paths, and the deposition areas are variables that can be simulated and predicted (e.g., with the 3 Distinct Element Method for stability analysis; Spreafico et al., 2014), preventing damages and casualties.

7. DISCUSSION AND CONCLUSIONS

The described landslides occurred, are occurring, and may occur in a relatively small, but densely inhabited area. Except for modelling, all the case studies are well known, with a vast literature that investigated them in-depth with different methods. Main approaches are summarized in Table 1, whilst the various aspects investigated for each landslide are gathered in Table 2. To avoid multiple repetitions, in this section the following acronyms will be used instead of the complete names of the landslides: MV (Masiere di Vedana), VJ (Vajont), TS (Tessina), and MP (Mt. Peron).

All case studies are strongly based on the investigation of the crown area, the detached rock mass, and the deposit. Similarly, field surveys and remote sensing have been adopted for all cases, but with different focus and methods.

It is quite reasonable that when dealing with past events (i.e., MV and VJ) the prime features to be investigated are the deposits. This is due both to the accessibility of the landslide mass, that usually lies in the valley

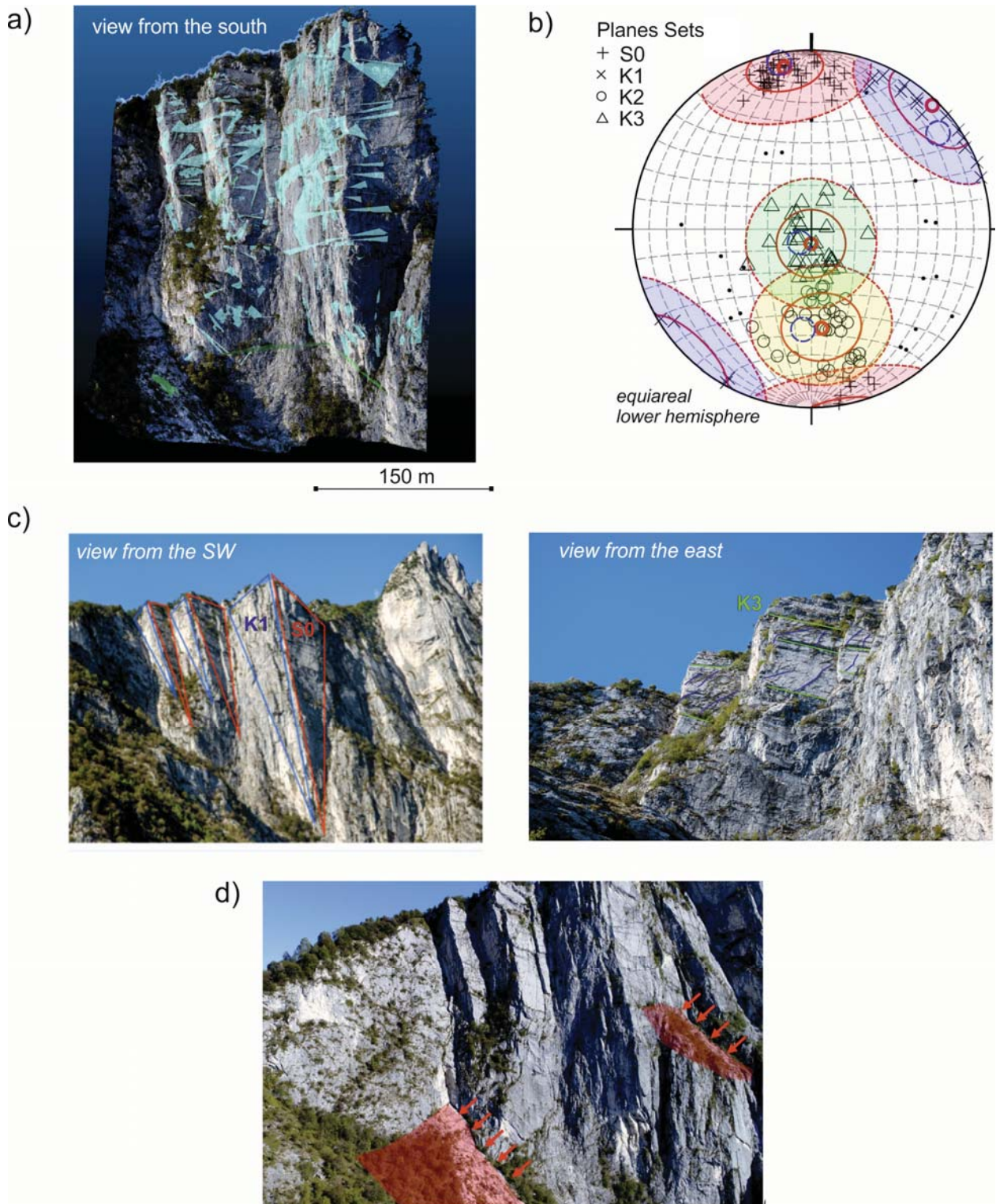


Fig. 16 - a) dense point cloud of the virtual outcrop and measured fracture planes (in blue); b) stereonet of the clustered data (poles to planes) with the resulting mean orientation of each cluster (red small circles), mean cone angle (red continuous line) and the external limit of each cluster (red dashed line); c) UAV-based imagery of the crown area with illustrative fractures sets highlighted; d) south-dipping planes ascribable to shear planes of the Mt. Peron backthrust (main planes are highlighted in red).

Method	Landslide name	Masiere di Vedana	Vajont	Tessina	Mt. Peron
Field survey		Extensive, main focus: the deposit	Extensive, main focus: the crown area and the deposit	Extensive, main focus: the crown area and the flanks	Very limited, main focus: bottom part of the crown area
Remote sensing		Aerial photos Digital elevation models	Digital elevation models	Aerial photo Historical photos Digital elevation models Photogrammetry Ground-based SAR interferometry	Drone photos Digital elevation models Photogrammetry
Bedrock stratigraphy		Yes	Yes	Yes	Yes
Bedrock structural characterization		Yes	Yes	Yes	Yes
Geomechanical characterization		Yes	Yes	Yes	Yes
Deposit analysis		Yes	Yes	Yes	Prediction
Dating		Isotopic dating Historical records Archaeology	Direct observation	Direct observation	No
Monitoring		No	No	Piezometers Inclinometers Multi-base wire extensometers Total stations Video cameras GNSS	No
Numerical modelling		2D distinct element method	Finite Element 3D distinct element Hybrid	Cellular automata SPH Finite difference	3D distinct element method

Tab. 1 - List of the methods applied in each case study. For each method is given a qualitative estimation of its accuracy and importance for the specific case study (high=green, medium=orange, poor=red).

bottom and may be easily sampled/investigated, and the difficulties that are encountered in reaching the crown. Looking at the Mt. Peron area this focus on deposit in such studies can be clearly appreciated. The southern side of this peak, an 800 m wide and about 700 m high rock wall, is the source area of the MV event but also hosts the rock prisms modelled in the MP. In both cases, the cliff has been investigated with remote sensing techniques and field surveys, but this phase is much more important in the MP case, compared to MV. In the former case, specifically designed photogrammetric surveys have been performed, to allow a virtual geomechanical characterization of the bedrock, the construction of a 3D model, and the identification of fracture planes in the rock wall. In the MV case, only field surveys were carried out to characterize the structural setting of the bedrock and to investigate the stratigraphic sequence, but little attention was devoted to specific present-day potential instabilities. On the contrary, the deposit was considered the most valuable source of information and many field surveys have been performed. VJ and TS are intermediate cases, having a quite accessible crown area where new detachments can take place. In the MV case, despite most investigations having been performed on the deposit, uncertainties remain, mostly because of the reworking processes that have taken place since the event, including anthropogenic activity. At the opposite extreme, the MP study focused on the source area and the pre-detachment geometry of the crown. The data acquired with this study are essential input values for numerical models focusing on the possible travel paths and deposition areas of future failures. Apart from the acquired input data, the precision and reliability of such numerical simulations depend solely on the adopted model itself.

The kinematics of a given landslide reflect directly

Landslide name	Masiere di Vedana	Vajont	Tessina	Mt. Peron
Source area	Estimated	Known	Known	Known
Travel path	Known	Known	Known	Known
Deposition area	Known	Known	Known	Known
Age	Known	Known	Known	Unknown
Driving factors	Supposed	Estimated	Estimated	Known
Trigger	Supposed	Known	Known	Supposed
Volume of the rock mass	Estimated	Estimated	Estimated	Known
Volume of the deposit	Estimated	Estimated	Estimated	Known
Pre-detachment geometry	Unknown	Known	Known	Known
Kinematic	Estimated	Estimated	Estimated	Known

Tab. 2 - List of the features describing each considered landslide. For each case is given a qualitative estimation of the accuracy (from the worst to the best: unknown, supposed, estimated, known) and reliability (high=green, medium=orange, poor=red) of the result.

on the land management of the area, but the identification of this parameter strongly relates to the age of the failure: the younger the event, the better its characterization. As it can be appreciated by looking also at Table 2, the actual moment of failure may be defined almost perfectly, if monitoring is ongoing when the event starts or people are affected by it (i.e., VJ and TS), or with an error up to some centuries, when absolute dating methods (e.g., ¹⁰Be or ¹⁴C) or historical records (i.e., MV) are used. In contrast, when dealing with future events like MP, the moment of failure may be totally unknown, depending on factors that cannot be completely estimated. The examples in this paper showed possible triggers of pore pressure increase (i.e., MV, VJ, and TS), and seismic shaking (i.e., MV, and MP), but many driving factors (e.g., fracturation of the rock mass, strata alternations, the presence of tectonic structures and fracture planes) have been identified. The comprehension of the stratigraphic, structural, and geomechanical characteristics of the rock mass proved to be essential to reconstruct

the dynamics of the failure in all case studies. The influence of a given parameter is connected to the specific setting, and the reliability of the final result may vary even in similarly investigated scenarios. Age plays an important role also in this case: the triggers of remote and future events are difficult to identify, and often no more than hypotheses can be proposed.

Disaster management in landslide-prone areas can be articulated in four different steps: mitigation, readiness, response, and recovery (Cartwright, 2005). Even a few minutes may be enough to activate emergency plans and save lives (e.g., Casagli et al., 2010; Manconi et al., 2016; Gallen et al., 2017). It is known that the accumulation of rock damage may be sufficient to reach the point of failure (e.g., Stead & Eberhardt, 2013; Donati et al., 2020). Some signs of movement can precede the collapse (e.g., Glastonbury & Fell, 2010) and, when a failure is considered possible, monitoring of the source area and/or the probable travel path can be activated, as in the VJ and TS cases. At VJ, piezometers and markers were placed within the landslide to monitor displacements and pore pressures immediately prior to the 1963 failure. At VJ, some signs preceding the event were present but were not correctly recognized, as occurred also in other cases (e.g., the Val Pola rock avalanche, 20th July 1987, and the Brenva ice avalanche, 18th January 1997). At TS, total station and GNSS monitoring is still active. GNSS provides values almost in real time, being able to vary the measuring interval in response to the trend of displacement. Other instrumentations have been placed at specific valuable sites (e.g., near the village of Funes), but the excessive costs and the need of continuous maintenance limit their application.

Early warning systems can be designed to alert the population and reduce landslide risk. Such systems are clearly site-specific, depending, for example, on the type of landslide (Lacasse & Nadim, 2009), but they are all based on the identification of the movement, the forecasting of the evolution of the event, the alert of the population, and the activation of response plans (Intrieri et al., 2012). Adequate prevention actions are pivotal to manage and to reduce casualties and damages to infrastructures (Casagli et al., 2010). Numerical modelling can help in the identification of the sectors of the slope where failure is more likely to occur, of the most probable travel path, and the potential runout distance of debris. The MP case is a clear example of state-of-the-art acquisition of data required for the modelling of possible instabilities, but also in all other cases numerical simulations have been performed. The VJ case perfectly highlights both the risk deriving from poor modelling based on poor input data (Ghirotti et al., 2013) and the continuous improvement in this field (Alonso & Pinyol, 2010; Paronuzzi & Bolla, 2012; Wolter et al., 2013, 2016; Franci et al., 2020a, 2020b).

Data deriving from real cases are fundamental to adjust numerical models and verify their output (e.g., Cola et al., 2019; von Wartburg et al., 2020). In this line, particular care should be dedicated to data collection for model inputs. A recommended approach should integrate field and remote-based techniques: the first provide data from close observations, not obtainable

through remote sensing (e.g., fracture opening or weathering) and constitute a ground-truth for remote sensing itself; the latter provide a spatially continuous distribution of data over a wider range of scales and offer the opportunity to test the 3D characterization of geological features (e.g., Pless et al., 2015). The understanding of real cases that occurred in the past is intertwined with modelling of future events, each aspect benefiting from improvements on the other one.

ACKNOWLEDGEMENTS

The authors are grateful to Dr Gianfranco Fioraso and an anonymous reviewer for their useful comments and suggestions, that significantly improved the quality of the paper. The authors deeply also thank the Editor, Dr Andrea Sposato.

REFERENCES

- Aaron J., McDougall S. (2019) - Rock avalanche mobility: the role of path material. *Engineering Geology*, 257, 105126.
Doi: 10.1016/j.enggeo.2019.05.003
- Abdulwahid W.M., Pradhan B. (2017) - Landslide vulnerability and risk assessment for multi-hazard scenarios using airborne laser scanning data (LiDAR). *Landslides*, 14(3), 1057-1076.
- Abele G. (1974) - Bergstürze in den Alpen. Ihre Verbreitung, Morphologie und Folgeerscheinungen. *Wiss. Alpenvereinshefte* 25, München.
- Alonso E.E., Pinyol N.M. (2010) - Criteria for rapid sliding I. A review of Vaiont case. *Engineering Geology*, 114 (3-4), 198-210.
Doi: 10.1016/j.enggeo.2010.04.018
- ARPAV (2018) - Technical report on the 27/10/2018 - 01/11/2018 meteorological event. regione.veneto.it/c/document_library/get_file?uuid=094022ae-43e7-46b1-86d2-ff3ebf669b89&groupId=90748
- Avolio M.V., Di Gregorio S., Mantovani F., Pasuto A., Rongo R., Silvano S., Stataro W. (2000) - Simulation of the 1992 Tessina landslide by a cellular automata model and future hazard scenarios. *Int. J. Appl. Earth Obs. Geoinf.*, 2 (1), 41-50.
- Bigi G., Cosentino D., Parotto M., Sartori R., Scandone P. (1990) - Structural model of Italy, scale 1: 500,000. CNR, Progetto Finalizzato Geodinamica, Firenze.
- Bowman E.T., Take W.A., Rait K.L., Hann C. (2012) - Physical models of rock avalanche spreading behaviour with dynamic fragmentation. *Canadian Geotechnical Journal*, 49(4), 460-476.
- Brideau M.A., Yan M., Stead D. (2009) - The role of tectonic damage and brittle rock fracture in the development of large rock slope failures. *Geomorphology*, 103 (1), 30-49.
- Carton A., Bondesan A., Fontana A., Meneghel M., Miola A., Mozzi P., Primon S., Surian N. (2009) - Geomorphological evolution and sediment transfer in the Piave River watershed (north-eastern Italy) since the LGM. *Géomorphologie: relief, processus, environnement*, 3, 37-58.
- Cartwright S. (2005) - National Civil Defence Emergen-

- cy Management Plan Order 2005. Published under the authority of the New Zealand Government, Wellington, New Zealand, pp. 68.
- Carulli G.B., Cozzi A., Longo Salvador G., Pernarcic E., Podda F., Ponton M. (2000) - Geologia delle Prealpi Carniche. Edizioni Museo Friulano di Storia Naturale, Udine, Italy, pp. 48.
- Casagli N., Catani F., Del Ventisette C., Luzi G. (2010) - Monitoring, prediction, and early warning using ground-based radar interferometry. *Landslides*, 7(3), 291-301.
- Cola S., Calabrò N., Pastor M. (2008) - Prediction of the flow-like movements of Tessina landslide by a SPH model. The 10th IS on Landslide and Engineering Slopes. Xi'an, China, vol. I, 647-653, Taylor, Francis, The Netherlands
- Cola S., Gabrieli F., Marcato G., Pasuto A., Simonini P. (2016) - Evolutionary behaviour of the Tessina landslide. *Rivista Italiana di Geotecnica*, 50(1), 51-79.
- Cola S., Brezzi L., Gabrieli F. (2019) - Calibration of rheological properties of materials involved in flow-like landslides. *Rivista Italiana Di Geotecnica*, (1), 5-43.
- Costa V., Doglioni C., Grandesso P., Masetti D., Pellegrini G.B., Tracanella E. (1996) - Note illustrative della Carta geologica d'Italia alla scala 1: 50.000: Foglio 063 - Belluno. Istituto Poligrafico e Zecca dello Stato, Roma.
- Crosta G.B., Chen H., Lee C.F. (2004) - Replay of the 1987 Val Pola landslide, Italian Alps. *Geomorphology*, 60(1-2), 127-146.
- D'Agostino N., Avallone A., Cheloni D., D'Anastasio E., Mantenuto S., Selvaggi G. (2008) - Active tectonics of the Adriatic region from GPS and earthquake slip vectors. *Journal of Geophysical Research*, 113, B12413.
- Dal Piaz G. (1912) - Studi geotettonici sulle Alpi orientali: regione fra il Brenta e i dintorni del lago di Santa Croce. Memorie dell'Istituto Geologico della Real Università di Padova, 1, 1-195.
- Dall'Olio L., Ghirotti M., Illiceto V., Semenza E. (1987) - La frana del Tessina - Alpago (BL). Proc. VI Congresso dell'Ordine Nazionale dei Geologi, Venezia, Italia, 275-293.
- Delvaux D., Sperner B. (2003) - Stress tensor inversion from fault kinematic indicators and focal mechanism data: the TENSOR program. Geological Society, London, Special Publications 212, 75-100.
- Di Giusto M. (2012) - Pericolosità indotta dalla caduta massi dal Monte Peron - Valutazione geologica. Technical evaluation for the municipality of Peron, Belluno, pp. 37.
- Dilley M. (2005) - Natural disaster hotspots: a global risk analysis, vol 5. World Bank Publications, pp. 148.
- Doglioni C. (1990) - The global tectonic pattern. *Journal of Geodynamics*, 12 (1), 21-38.
- Donati D., Stead D., Lato M., Gaib S. (2020) - Spatio-temporal characterization of slope damage: Insights from the Ten Mile Slide, British Columbia, Canada. *Landslides*, 17, 1037-1049.
- Dykes A.P., Bromhead E.N. (2018a) - The Vaiont landslide: re-assessment of the evidence leads to rejection of the consensus. *Landslides*, 15(9), 1815-1832.
- Dykes A.P., Bromhead E.N. (2018b) - New, simplified and improved interpretation of the Vaiont landslide mechanics. *Landslides*, 15(10), 2001-2015.
- Eisbacher G.H., Clague J.J. (1984) - Destructive mass movements in high mountains: hazard and management, Geological Survey of Canada, Vancouver, British Columbia, Canada, pp. 230.
- Franci A., Cremonesi M., Perego U., Crosta G., Oñate E. (2020a) - 3D simulation of Vajont disaster. Part 1: Numerical formulation and validation. *Engineering Geology*, 279, 105854. Doi: 10.1016/j.enggeo.2020.105854
- Franci A., Cremonesi M., Perego U., Oñate E., Crosta G. (2020b) - 3D simulation of Vajont disaster. Part 2: Multi-failure scenarios. *Engineering Geology*, 279, 105856. Doi: 10.1016/j.enggeo.2020.105856
- Friedmann S.J., Kwon G., Losert W. (2003) - Granular memory and its effect on the triggering and distribution of rock avalanche events. *Journal of Geophysical Research: Solid Earth*, 108 (B8).
- Gabrieli F., Corain L., Vettore L. (2016) - A low-cost landslide displacement activity assessment from time-lapse photogrammetry and rainfall data: Application to the Tessina landslide site. *Geomorphology*, 269, 56-74.
- Galadini F., Poli M.E., Zanferrari A. (2005) - Seismogenic sources potentially responsible for earthquakes with $M \geq 6$ in the eastern Southern Alps (Thiene-Udine sector, NE Italy), *Geophys. J. Int.*, 161 (3), 739-762.
- Gallen S.F., Clark M.K., Godt J.W., Roback K., Niemi A. (2017) - Application and evaluation of a rapid response earthquake-triggered landslide model to the 25 April 2015 Mw 7.8 Gorkha earthquake, Nepal. *Tectonophysics*, 714, 173-187.
- Genevois R., Armento C., Tecca P.R. (2006) - Failure mechanisms and runout behaviour of three rock avalanches in the north-eastern Italian Alps. In: Evans S.G., Mugnozza G.S., Strom A., Hermanns R.L. (eds) *Landslides from Massive Rock Slope Failure*. NATO Science Series 49. Springer, Dordrecht, 407-427.
- Ghirotti M., Masetti D., Massironi M., Oddone E., Sapigni M., Zampieri D., Wolter A. (2013) - The 1963 Vajont landslide (Northeast Alps, Italy): post-conference field trip (October 10th, 2013). In: Genevois R., Prestininzi A. (eds) *International Conference on Vajont - 1963-2013: thoughts and analyses after 50 years since the catastrophic landslide*. Italian Journal of Engineering Geology and Environment - Book Series No. 6, 635-646, Sapienza Università Editrice, Rome, Italy.
- Ghirotti M., Borgatti L., Marcato G. (2020) - One of the hazardous neighbours of the Vajont landslide: the historical Mt. Salta rock avalanche. *Alpine and Mediterranean Quaternary*, 33, 2, 157-164. Doi: 10.26382/AMQ.2020.11
- Gischig V., Preisig G., Eberhardt E. (2016) - Numerical investigation of seismically induced rock mass fatigue as a mechanism contributing to the progressive failure of deep-seated landslides. *Rock Mechanics and Rock Engineering*, 49(6), 2457-2478.

- Glastonbury J., Fell R. (2010) - Geotechnical characteristics of large rapid rock slides. *Canadian Geotechnical Journal*, 47, 116-132.
- Heim A. (1932) - *Bergsturz und Menschenleben*. Vierteljahrsschr. Naturf. Ges. Zürich 20, Beer & Co., Zurich, pagine?.
- Hendron A.J., Patton F.D. (1985) - The Vaiont Slide, a Geotechnical Analysis Based on New Geologic Observations of the Failure Surface. Technical Report GL-85-5, U.S. Army Eng. Waterways Experiment Station, I, II, Vicksburg, MS, pp. 259.
- Hermanns R.L., Longva O. (2012) - Rapid rock-slope failures, in: *Landslides (types, mechanisms and modeling)*, edited by: Clague, J. J., and Stead, D., Cambridge University Press, Cambridge, UK, 59-70.
- Herrera G., Mateos R.M., García-Davalillo J.C. et al. (2018) - Landslide databases in the Geological Surveys of Europe. *Landslides*, 15, 359-379.
- Hervás J., Barredo J.I., Rosin P.L., Pasuto A., Mantovani F., Silvano S. (2003) - Monitoring landslides from optical remotely sensed imagery: the case history of Tessina Landslide, Italy. *Geomorphology*, 54(1-2), 63-75.
- Hoernes R. (1892) - Der Querbruch von Santa Croce und die Bildung der Schuttmassen von Cima Fadalto und der Rovine di Vedana bei Belluno. *Zeitschrift der Deutschen Geologischen Gesellschaft*, 347-351.
- Hungr O. (2006) - Rock avalanche occurrence, process and modelling. In: *Landslides from Massive Rock Slope Failure*, edited by: Evans S.G., Scarascia-Mugnozza G., Strom A.L., Hermanns R.L.. NATO Science Series, 49, 243-266.
- Hungr O., Evans S.G., Hutchinson I.N. (2001) - A Review of the Classification of Landslides of the Flow Type. *Environmental & Engineering Geoscience*, 7 (3), 221-238.
Doi: 10.2113/gseegeosci.7.3.221
- Intrieri E., Gigli G., Mugnai F., Fanti R., Casagli N. (2012) - Design and implementation of a landslide early warning system. *Engineering Geology*, 147, 124-136.
- ISPRA (2018) - Consumo di suolo, dinamiche territoriali e servizi ecosistemici. *Rapp. 288/2018*, pp. 280. ISBN: 978-88-448-0902-7
- Lacasse S., Nadim F. (2009) - Landslide risk assessment and mitigation strategy. In: Sassa K., Canuti P. (Eds.), *Landslides-Disaster Risk Reduction*. Springer Verlag, Berlin Heidelberg, 31-61.
- MacQueen J. (1967) - An enriched K-means clustering method for grouping fractures with meliorated initial centers. Some methods for classification and analysis of multivariate observations. *Proceedings of the fifth Berkeley symposium on mathematical statistics and probability*. California, USA, p. 14.
- Manconi A., Picozzi M., Coviello V., De Santis F., Elia, L. (2016) - Real-time detection, location, and characterization of rockslides using broadband regional seismic networks. *Geophysical Research Letters*, 43 (13), 6960-6967.
- Mangeny A., Roche O., Hungr O., Mangold N., Faccanoni G., Lucas A. (2010) - Erosion and mobility in granular collapse over sloping beds. *Journal of Geophysical Research: Earth Surface*, 115, F03040.
- Marzolf I., Poesen J. (2009) - The potential of 3D gully monitoring with GIS using high-resolution aerial photography and a digital photogrammetry system. *Geomorphology*, 111 (1-2), 48-60.
Doi: 10.1016/j.geomorph.2008.05.047
- Montandon F. (1933) - Chronologie des grands éboulements alpins du début de l'ère chrétienne à nos jours. *Matériaux pour l'étude des calamités*, 32, 271-340.
- Mantovani F., Pasuto A., Silvano S., Zannoni A. (2000) - Collecting data to define future hazard scenarios of the Tessina landslide. *Int. J. Appl. Earth Obs. Geoinf.*, 2(1), 33-40.
- Martin S., Ivy-Ochs S., Viganò A., Campedel P., Rigo M., Vockenhuber C., Gabrieli F., Mair V., Rossato S. (2020) - Landslides of the western Dolomites: case studies from the Adige and Sarca Valleys (NE Italy). *Alpine and Mediterranean Quaternary*, 33, 2, 191-207.
Doi: 10.26382/AMQ.2020.15
- Márton E., Drobne K., Čosović V., Moro A. (2003) - Palaeomagnetic evidence for Tertiary counterclockwise rotation of Adria. *Tectonophysics*, 377(1-2), 143-156.
- Massey C.I., McSaveney M.J., Taig T., Richards L., Litchfield N.J., Rhoades D.A., McVerry G.H., Lukovic B., Heron D.W., Ries W., Van Dissen R.J. (2014) - Determining rockfall risk in Christchurch using rockfalls triggered by the 2010-2011 Canterbury earthquake sequence. *Earthquake Spectra*, 30 (1), 155-181.
- Massironi M., Zampieri D., Superchi L., Bistacchi A., Ravagnan R., Bergamo A., Ghirotti M., Genevois R. (2013) - Geological structures of the Vajont landslide. *Italian Journal of Engineering Geology and Environment - Book Series*, (6), 573-582.
- Mazzuoli L. (1875) - *Sull'origine delle rovine di Vedana*. Club Alpino Italiano, sez. di Agordo, Adunanza straordinaria dei soci il 22-8-1875 in Vedana, 11-17.
- Miari F. (1830) - *Compendio storico della regia città di Belluno e sua antica provincia*. Giuseppe Picotti, Venezia, pp. 144.
- Monegato G., Scardia G., Hajdas I., Rizzini F., Piccin A. (2017) - The Alpine LGM in the boreal ice-sheets game. *Scientific reports*, 7(1), 1-8.
- More K.S., Wolkersdorfer C. (2019) - An analogue Toma Hill formation model for the Tyrolian Fernpass rockslide. *Landslides*, 16, 1855-1870.
- Nicoletti P.G., Sorriso-Valvo M. (1991) - Geomorphic controls of the shape and mobility of rock avalanches. *Geol. Soc. Am. Bull.*, 103 (10), 1365-1373.
- Parker R., Petley D., Densmore A., Rosser N., Dambly D., Brain M. (2013) - Progressive failure cycles and distributions of earthquake-triggered landslides. In: Ugai K., Yagi H., Wakai A. (eds) *Earthquake-Induced Landslides*. Springer, Berlin, Heidelberg, 755-762.
- Paronuzzi P., Bolla A. (2012) - The prehistoric Vajont rockslide: an updated geological model. *Geomorphology*, 169-170, 165-191
- Pasuto A. (2017) - The Vajont Valley (Eastern Alps): A Complex Landscape Deeply Marked by Landsliding. In M. Soldati and M. Marchetti (eds.), *Landscapes*

- and Landforms of Italy, World Geomorphological Landscapes, 135-145.
- Pasuto A., Silvano S. (1995) - The Tessina landslide. In: Horlick Jones, T., Amendola, A., Casale, R. (Eds.), *Natural Risk and Civil Protection*. Chapman & Hall, London.
- Pellegrini G.B. (ed) (2000) - Note illustrative della Carta Geomorfologica d'Italia - Foglio Belluno. Regione Veneto - Servizio Geologico d'Italia, pp. 141.
- Pellegrini G.B., Surian N., Albanese D. (2006) - Landslide activity in response to alpine deglaciation: the case of the Belluno Prealps (Italy). *Geografia Fisica e Dinamica Quaternaria*, 29, 185-196.
- Piloni G. (1607) - *Historia della Città di Belluno*. Venezia, pp. 634.
- Pless J.C., McCaffrey K. J.W., Jones R.R., Holdsworth R.E., Conway A., Krabbendam M. (2015) - 3D characterization of fracture systems using terrestrial laser scanning: An example from the Lewisian basement of NW Scotland. *Geological Society, London, Special Publications*, 421(1), 125-141.
- Preisig G., Gischig V., Eberhardt E., Hungr O. (2015) - Hydromechanical versus seismic fatigue in progressive failure of deep-seated landslides. In: 13th ISRM International Congress of Rock Mechanics. International Society for Rock Mechanics and Rock Engineering.
- Riva M., Besio M., Masetti D., Roccati F., Sapigni M, Semenza E. (1990) - Geologia delle Valli Vaiont e Gallina (Dolomiti orientali). *Annali Università di Ferrara (Sezione Scienze Geologiche e Paleontologiche)*, 2(4), 55-76.
- Rossato S., Fontana A., Mozzi P. (2015) - Meta-analysis of a Holocene 14 C database for the detection of paleohydrological crisis in the Venetian-Friulian Plain (NE Italy). *Catena*, 130, 34-45.
- Rossato S., Martin S., Ivy-Ochs S., Viganò A., Vockenhuber C., Rigo M., Surian N., Mozzi P. (2018) - Post-LGM catastrophic landslides in the Dolomites: when, where and why. *Alpine and Mediterranean Quaternary*, 31 (2), 239-242.
- Rossato S., Ivy-Ochs S., Martin S., Viganò A., Vockenhuber C., Rigo M., Monegato G., De Zorzi M., Surian N., Campedel P., Mozzi P. (2020) - Timing, drivers and impacts of the historic Masiere di Vedana rock avalanche (Belluno Dolomites, NE Italy). *Nat. Hazards Earth Syst. Sci.*, 20, 2157-2174. Doi: 10.5194/nhess-20-2157-2020
- Samia J., Temme A., Bregt A., Wallinga J., Guzzetti F., Ardizzone F., Rossi M. (2017) - Do landslides follow landslides? Insights in path dependency from a multi-temporal landslide inventory, *Landslides*, 14 (2), 547-558.
- Schuster R.L., Wieczorek G.F. (2002) - Landslide triggers and types. In: Rybár J., Stemberk J., Wagner P. (eds) *Landslides: proceedings of the first European conference on landslides*. Taylor & Francis, Prague, 59-78.
- Selli R., Trevisan L., Carloni C.G., Mazzanti R., Ciabatti M. (1964) - La Frana del Vaiont. *Giornale di Geologia*, XXXII(1), 1-154.
- Semenza E. (2010) - The Story of Vaiont told by the Geologist who Discovered the Landslide. K-flash, Ferrara. www.k-flash.it
- Semenza E., Ghirotti M. (2000) - History of 1963 Vaiont Slide. The importance of the geological factors to recognise the ancient landslide. *Bull. Eng. Geol. Env.*, 59, 87-97.
- Spreafico M.C., Francioni M., Cervi F., Stead D., Bitelli G., Ghirotti M., Girelli V.A., Lucente C.C., Tini M.A., Borgatti L. (2014) - Back Analysis of the 2014 San Leo Landslide Using Combined Terrestrial Laser Scanning and 3D Distinct Element Modelling. *Rock Mechanics and Rock Engineering*, 49, 2235-2251. Doi: 10.1007/s00603-015-0763-5
- Squinabol S. (1902) - *Venti giorni sui Monti Bellunesi*. Tip. Raffaello Giusti, Livorno, pp. 52.
- Stead D., Eberhardt E. (2013) - Understanding the mechanics of large landslides. *Italian Journal of Engineering Geology and Environment - Book Series*, 6, 85-112.
- Stead D., Wolter A. (2015) - A critical review of rock slope failure mechanisms: the importance of structural geology. *Journal of Structural Geology*, 74, 1-23.
- Stefani C., Fellin M.G., Zattin M., Zuffa G.G., Dalmonte C., Mancin N., Zanferrari A. (2007) - Provenance and paleogeographic evolution in a multi-source foreland: the Cenozoic Venetian-Friulian Basin (NE Italy). *Journal of Sedimentary Research*, 77(11), 867-887.
- Strom A. (2006) - Morphology and internal structure of rockslides and rock avalanches: grounds and constraints for their modelling, in: *Landslides from Massive Rock Slope Failure*, edited by: Evans S.G., Mugnozza G.S., Strom A., Hermanns R.L., NATO Sci. S., 49, 305-326.
- Superchi L., Floris M., Ghirotti M., Genevois R., Jaboyedoff M., Stead D. (2010) - Technical note: implementation of a geodatabase of published and unpublished data on the catastrophic Vaiont landslide. *Nat Hazards Earth Syst Sci*, 10, 865-873.
- Takahashi T. (2001) - Process of occurrence, flow and deposition of viscous debris flow. In: Seminara G., Blondeaux P. (eds) *River, Coastal and Estuarine Morphodynamics*. Springer, Berlin, 93-118. Doi: 10.1007/978-3-662-04571-8_5
- Taramelli T. (1883) - Note alla Carta Geologica della Provincia di Belluno. Ed. Fusi, Pavia, pp. 215.
- Tarchi D., Casagli N., Fanti R., Leva D.D., Luzi G., Pasuto A., Pieraccini M., Silvano S. (2002) - Landslide monitoring by using ground-based SAR interferometry: an example of application to the Tessina landslide in Italy. *Engineering Geology*, 68, 15-30.
- Travelletti J., Delacourt C., Allemand P., Malet J.-P., Schmittbuhl J., Toussaint R., Bastard M. (2012) - Correlation of multi-temporal ground-based optical images for landslide monitoring: Application, potential and limitations. *ISPRS Journal of Photogrammetry and Remote Sensing*, 70, 39-55. Doi: 10.1016/j.isprsjprs.2012.03.007
- Trigila A., Iadanza C., Guerrieri L. (2007) - The IFFI project (Italian landslide inventory): Methodology and results, in: *Guidelines for Mapping Areas at Risk of Landslides in Europe*, edited by: Hervás, J., 15-

- 18.
- Trigila A., Iadanza C., Bussetini M., Lastoria B. (2018) - Dissesto idrogeologico in Italia: pericolosità e indicatori di rischio. Edizione 2018, ISPRA, Rapporti 287/2018.
- Van Westen C.J., Lulie Getahun F. (2003) - Analyzing the evolution of the Tessina landslide using aerial photographs and digital elevation models. *Geomorphology*, 54(1-2), 77-89.
- Venzo S. (1939) - Osservazioni geotettoniche e geomorfologiche sul rilevamento del Foglio Belluno. *Bollettino della Società Geologica Italiana*, 58, 433-451.
- von Wartburg J., Ivy-Ochs S., Aaron J.B., Martin S., Leith K., Rigo M., Vockenhuber C., Campedel P., Viganò A. (2020) - Constraining the age and source area of the Molveno landslide deposits in the Brenta Group, Trentino Dolomites (Italy). *Frontiers in Earth Science*, 8, 164.
- Westoby M.J., Brasington J., Glasser N.F., Hambrey M.J., Reynolds J.M. (2012) - Structure-from-Motion photogrammetry: A low-cost, effective tool for geoscience applications. *Geomorphology*, 179, 300-314.
- Wieczorek G.F. (1996) - Landslide triggering mechanisms. In: Turner A.K., Schuster R.L. (eds) *Landslides: Investigation and Mitigation*. Transportation Research Board, National Research Council, Special Report, Washington DC, 76-90.
- Wirth S.B., Glur L., Gilli A., Anselmetti F.S. (2013) - Holocene flood frequency across the Central Alps - solar forcing and evidence for variations in North Atlantic atmospheric circulation. *Quaternary Science Reviews*, 80, 112-128.
- Wolter A., Havaej M., Zorzi L., Stead D., Clague J.J., Ghirotti M., Genevois R. (2013) - Exploration of the kinematics of the 1963 Vajont slide, Italy, using a numerical modelling toolbox. *Ital J Eng Geol Environ*, 6, 599-612.
- Wolter A., Stead D., Clague J.J. (2014) - A morphologic characterisation of the 1963 Vajont Slide, Italy, using long-range terrestrial photogrammetry. *Geomorphology*, 206, 147-164.
- Wolter A., Stead D., Ward B.C., Clague J.J., Ghirotti M. (2016) - Engineering geomorphological characterisation of the Vajont slide, Italy, and a new interpretation of the chronology and evolution of the landslide. *Landslides*, 13, 1067-1081.
- Zanferrari A., Masetti D., Monegato G., Poli M.E. (2013) - Geological map and explanatory notes of the Geological Map of Italy at the scale 1:50.000: Sheet 049 "Gemona del Friuli". ISPRA - Servizio Geologico d'Italia - Regione Autonoma Friuli-Venezia Giulia, pp. 262.